



AIAA 2001-4067

**A Monte Carlo Dispersion Analysis
of the X-33 Simulation Software**

Peggy S. Williams
NASA Dryden Flight Research Center
Edwards, California

AIAA Atmospheric Flight Mechanics Conference
August 6–9, 2001
Montreal, Canada

For permission to copy or to republish, contact the copyright owner named on the first page.

For AIAA-held copyright, write to AIAA Permissions Department,
1801 Alexander Bell Drive, Suite 500, Reston, Virginia 22091-4344.

A MONTE CARLO DISPERSION ANALYSIS OF THE X-33 SIMULATION SOFTWARE

Peggy S. Williams*
NASA Dryden Flight Research Center
Edwards, California

Abstract

A Monte Carlo dispersion analysis has been completed on the X-33 software simulation. The simulation is based on a preliminary version of the software and is primarily used in an effort to define and refine how a Monte Carlo dispersion analysis would have been done on the final flight-ready version of the software. This report gives an overview of the processes used in the implementation of the dispersions and describes the methods used to accomplish the Monte Carlo analysis. Selected results from 1000 Monte Carlo runs are presented with suggestions for improvements in future work.

q	dynamic pressure
RCS	reaction control system
v	velocity, kn
x_{cg}	horizontal position location of the center of gravity, ft
y_{cg}	vertical position location of the center of gravity, ft
α	angle of attack, deg
σ	standard deviation

Nomenclature

E	total energy
FADS	flush airdata sensing
g	gravitational constant, 32.2 ft/sec ²
GRAM	global reference atmospheric model
h	altitude, ft
HAC	heading alignment cone
INS/GPS	inertial navigation system/global positioning system
ITF	Integration and Test Facility
m	mass
P_{hit}	probability of a "hit" (a successful landing)
P_{miss}	probability of a "miss" (a failed landing)

Introduction

The X-33 vehicle was designed for the NASA access-to-space program by Lockheed Martin Skunk Works (Palmdale, California) as a subscale prototype of a reusable launch vehicle. The NASA access-to-space program encourages industry partners to develop space vehicles that reduce the cost of putting a payload into orbit. The X-33 vehicle was designed as a single-stage-to-orbit technology demonstrator to prove new technologies for future use in second-generation and subsequent reusable launch vehicle programs. Some key technologies that would have been demonstrated by the X-33 vehicle include the reusable launch vehicle operations concept; propellant tanks and thermal protection system technologies; airframe and structure technologies; and advances in the propulsion, aerodynamics, and vehicle subsystems.¹

The X-33 vehicle was designed to be vertically launched from Edwards Air Force Base in California and autonomously horizontally land at Michael Army Airfield in Utah. The 12-min flight would consist of several flight phases, each phase having independent guidance and control laws. The flight phases, in order of occurrence, are launch or liftoff, ascent, main engine cutoff, transition, entry or descent, terminal area energy management, approach and landing, touchdown, and rollout. The X-33 vehicle was designed to be unmanned,

*Aerospace Engineer

Copyright © 2001 by the American Institute of Aeronautics and Astronautics, Inc. No copyright is asserted in the United States under Title 17, U.S. Code. The U.S. Government has a royalty-free license to exercise all rights under the copyright claimed herein for Governmental purposes. All other rights are reserved by the copyright owner.

reach a suborbital altitude of approximately 200,000 ft, and fly at speeds to a maximum of Mach 10.3.

Testing of the X-33 flight control system has been complemented with a Monte Carlo simulation analysis of the X-33 mission trajectory. This type of testing ensures that adequate margins (control, thermal, structural, and so forth) exist throughout the flight envelope. The X-33 nonlinear six-degree-of-freedom high-fidelity batch simulation was used to repeatedly fly a specific mission profile. No intervention was required to simulate a complete trajectory because the vehicle was completely autonomous. This autonomy allows multiple runs to be directly compared.

The Monte Carlo method of dispersion analysis uses a given system model (in this case, the X-33 flight control system) and introduces statistical uncertainties on as many of the individual mathematical models (for example, aerodynamics, propulsion, actuators, propellants, winds) as practical. These uncertainties were categorized for this analysis using a Gaussian distribution, with the magnitude of each uncertainty defined as one standard deviation ($1-\sigma$) value from the nominal value. Atmospheric and wind uncertainties were based on a set of known observations and had a randomly selected value from the set of known observations, such as launch wind conditions for each run. All other categories of uncertainties were considered to be normally distributed, with a zero mean.

Normally distributed random gains (with zero mean and a standard deviation of 1) were selected and multiplied the $1-\sigma$ uncertainty value before being applied to the simulation parameters. Each Monte Carlo simulation run had a different random variation of the dispersions. The dispersions used in the Monte Carlo simulations were applied to the X-33 vehicle dynamics, navigation systems, and external environment models.

The number of Monte Carlo runs containing uncertainty combinations that result in failure to complete the mission were identified; thus, the probability of mission success was established. Although establishing the probability of mission success was one of the primary goals of this analysis, other objectives such as validation of the avionics system and hazard and risk mitigation also were accomplished. Completing the Monte Carlo analysis also allowed for the identification of design weaknesses in guidance or control, trajectory, and margins in specific aircraft parameters.

The objective of this report is to demonstrate how Monte Carlo simulation analysis can be used to identify and analyze guidance, control, and trajectory problems for an autonomous vehicle and to provide some preliminary results for the X-33 vehicle. Results are presented for selected conditions at touchdown for the 1000 Monte Carlo runs done in this analysis and compared to the successful landing criteria for the vehicle. Liquid oxygen weight margins at touchdown are provided to aid in future trajectory modifications. A dispersion plot of lateral runway position at touchdown exemplifies how the Monte Carlo dispersion analysis can help locate problems in the guidance or control portion of the software.

Landing trajectories for several of the Monte Carlo runs are presented and discussed. The effect of individual dispersions on the vehicle in flight is discussed using the examination of two failed dispersion runs. In examination of other runs, total energy of the vehicle is correlated to the landing trajectory of the vehicle. Possible extensions of this type of energy analysis and other slated future work are also discussed.

Note that use of trade names or names of manufacturers in this document does not constitute an official endorsement of such products or manufacturers, either expressed or implied, by the National Aeronautics and Space Administration.

Vehicle Description

The X-33 vehicle has a lifting-body shape and is designed to be powered by two linear aerospike engines, each capable of producing 205,000 lbf of thrust, that use a propellant mixture composed of liquid hydrogen and liquid oxygen. The vehicle has a range of 950 mi, an empty weight of 75,000 lb, and a maximum weight of 285,000 lb when fully load with fuel. The vehicle has a span of 77 ft, a length of 69 ft, and a height of 22 ft, 4 in. The vehicle has eight control surfaces: two body flaps, four elevons, and two rudders. The vehicle also is designed to use reaction control system (RCS) thrusters for added vehicle control during unpowered flight. Figure 1 shows the current vehicle configuration.

The X-33 Simulation

The X-33 software simulation used in this analysis was developed at the Integration and Test Facility (ITF) located at the NASA Dryden Flight Research Center (Edwards, California). The primary role of the ITF in the X-33 project has been to provide mission simulation capabilities. The ITF was also used in the hardware and



EC99-44921-1

Figure 1. The X-33 advanced technology demonstrator.

software integration process and mission planning and was to be used for hardware-in-the-loop integration, flight test support, hazard and risk reduction, and range network integration.

The ITF X-33 simulation is a six-degree-of-freedom high-fidelity simulation that has many components. The core components include the aerodynamics, aerothermal, mass properties, equations of motion, and structural dynamics models. Other components of the simulation are the environment (containing models of the atmosphere, surface winds, winds aloft, gust, radio frequency blackout, gravity, and terrain) and the avionics system (including the guidance laws, flush airdata sensing (FADS) system, mission manager, inertial navigation system/global positioning system (INS/GPS), and vehicle health monitor). Subsystem components include a landing gear model, and models for the brakes and steering system, power distribution, propellant sensors, the RCS, the main propulsion system controller, the active thermal control system, the purge/vent system, and the actuator.

Dispersion Models

The dispersions used in the Monte Carlo simulations have been applied to the vehicle dynamics, navigation systems, and external environment models. The models modified in the X-33 simulation to include dispersion capabilities were the aerodynamics, mass properties, navigation processing, engine, RCS, propellant sensor, aerothermal, and atmospheric models. A description of each of the dispersion models used in this analysis is provided in the following paragraphs. Information is

given regarding how the uncertainties were determined and how specific parameters in each of the models were modified to include the uncertainties. Dispersions were applied throughout the entire flight trajectory unless otherwise indicated. In most cases, dispersion values applied also varied as a function of flight condition.

The 1- σ dispersion values were obtained by referring to a document provided by Lockheed-Martin.[†] Figure 2 shows the categories of dispersions defined in the document[†] and the corresponding numbers of total dispersions in each category. The X-33 program would have tested to 2- σ dispersions when testing the final flight-ready version of software. The analysis discussed in this report tested over the entire normal distribution mainly to ensure that enough failure cases would be generated for analysis. Rare cases of high dispersion values can sometimes be generated that are outside of the expected 3- σ defined dispersion range; this analysis did not discard those values.

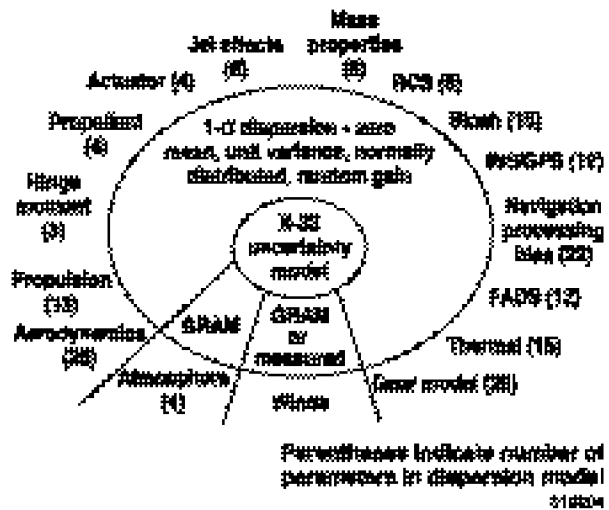


Figure 2. Dispersion models.[†]

Aerodynamics

The aerodynamics model calculates aerodynamic coefficient and stability derivatives that are functions of Mach number, angle of attack (α), angle of sideslip, and surface deflections of the vehicle. The aerodynamic uncertainties are based on comparisons between historical flight measurements and preflight predictions

[†]Lockheed Martin Skunk Works, "X-33 Dispersions Document," 604D0122_A, self-published (generated under NASA Cooperative Agreement No. NCC 8-73), 1999.

of other lifting-body and hypersonic aircraft. The preflight predictions were based on wind-tunnel data.

Additionally, a statistical analysis of the X-33 wind tunnel data was used to further improve and define aerodynamic uncertainties. The $1-\sigma$ value was estimated for each aerodynamic coefficient; uncertainty values could then be added to each coefficient during the simulation. The aerodynamic uncertainty dispersion models had the ability to disperse 26 aerodynamic coefficients and the lift-to-drag-ratio.

Jet Effects

Jet effects are the incremental change in vehicle forces and moments between the condition in which engine plume is present and the condition in which no engine plume is present. The uncertainty values apply to nozzle pressure ratio, control surface deflection, or engine thrust-vectoring angle. The dispersion values are based on a table lookup that is a function of Mach number. Uncertainties are estimated on six parameters: lift, drag, and side forces and pitch, roll, and yaw moments. The uncertainty data for jet effects were calculated from repeated runs of the jet effects in wind-tunnel tests.

Hinge Moments

The hinge moment model provides hinge moment data that are a function of Mach number, α , angle of sideslip, and surface deflection. The hinge moment uncertainty data are defined by the actuator manufacturer. The uncertainty model data are a function of Mach number, α , and surface deflection. The hinge moment model has three uncertainty parameters, one for each of the three control surfaces: body flap, rudder, and elevon.

Mass Properties

The mass properties model of the X-33 vehicle contains inertia, center of gravity, and weight as a function of total fuel levels, fuel fractions, and vehicle attitude. In practice, the weight and longitudinal and lateral center of gravity are determined by weighing the vehicle. The uncertainty in inert mass is caused by the scale calibration tolerance and is a “worst-case” number based on the assumption that all three scales are reading maximum tolerance on the same side of nominal. The uncertainties in the inert horizontal and vertical position locations of the center of gravity (x_{cg} and y_{cg} , respectively) also are worst-case numbers derived from the scale tolerance. The worst-case conditions for these data based on the actual weight of the X-33 vehicle are all mutually exclusive.

Navigation Processing

Navigation processing includes dispersions of the INS/GPS system and the radar altimeter. The FADS dispersions also are part of navigation processing but have not been implemented into the simulation. The INS/GPS dispersions are on position, velocity, body acceleration, body rates, pitch and roll Euler angles, and heading angle. For the radar altimeter, a dispersion is available on altitude.

Engine

Engine dispersions include aerodynamic forces and moments that are a function of pressure altitude. Fuel flow rate, oxidizer flow rate, and the mixture ratio dispersion are all constant values generated by the engine manufacturer for the linear aerospike engine. The uncertainty value for the engine installation mounting alignment was also a constant.

Propellant

The models for the liquid oxygen and liquid hydrogen tanks simulate pressure, temperature, and mass dynamics. The tank physics can be described in terms of the major influences on residual gas pressure inside the tank and the fill status of the tank within an accelerating inertial environment. Propellant dispersions were given as a percentage of uncertainty in the ability to control the initial amount of loading of liquid hydrogen and liquid oxygen in the tanks. To incorporate the dispersions in the residual amounts of liquid oxygen and liquid hydrogen, the sensor location for liquid oxygen was moved an appropriate amount to correspond to the uncertainty value given. To incorporate the liquid hydrogen residual amount dispersion, the density of hydrogen was changed to correspond to the uncertainty value given in the residual amount of liquid hydrogen.

Atmospheric

Two combinations of atmospheric dispersions methods originally integrated in the X-33 simulation were available for use in this Monte Carlo dispersion analysis. First, the ability to implement the global reference atmospheric model (GRAM)² with and without winds was used. The GRAM is an engineering model atmosphere that includes mean values for density, temperature, pressure, and wind components, in addition to random perturbation profiles for density variations along a specified trajectory. The atmospheric data are a function of latitude, longitude, altitude, and day of the year.³

An alternate source for winds was a simple winds table that is present in the current X-33 simulation. Although defined in the document previously mentioned,[‡] aerothermal and aerosurface actuation dispersions were not incorporated into the X-33 simulation or the Monte Carlo analysis described in this paper.

Methods Of Approach

Monte Carlo analysis estimates the statistics of random variables by analyzing the statistics of many trials. One important question associated with Monte Carlo analysis is determining the number of trials needed before the statistics of a variable can be estimated with reasonable accuracy. Considering a single run of the simulation to be either successful (a “hit”) or unsuccessful (a “miss”) based on predetermined criteria allows each run of the simulation to be treated as a discrete, two-state, random variable. The estimation uncertainty in the Monte Carlo method can be quantified when estimating the statistics of discrete, two state, random variables.[‡] Table 1 shows the estimation uncertainties calculated by Lintereur in an unpublished paper.[‡]

Table 1. Number of Monte Carlo trials required to achieve a desired estimation uncertainty with known probability.[‡]

Uncertainty probability range	Number of Monte Carlo trials based on percent of estimation uncertainty				
	20%	15%	10%	5%	1%
0 → 0.683	7	12	25	100	2,500
0.750 → 0.954	25	45	100	400	10,000
0.890 → 0.997	57	100	225	900	22,500
0.940 → 0.999	100	178	400	1,600	40,000

The assumptions made in completing the calculations herein were that the Monte Carlo trials are statistically independent, the uncertainty probability range lower bound is given by Chebyshev inequality, and the uncertainty probability range upper bound is given by the central limit theorem. Variance of the Monte Carlo estimate is determined by multiplying the probability of a hit, P_{hit} , by the probability of a miss, P_{miss} . The worst-case variance (the case where the variance is the

largest it can possibly be) occurs when $P_{hit} = 0.5$ and $P_{miss} = 0.5$, which produces a variance of 0.25. This assumption of worst-case variance was made by Lintereur to form table 1.

An intuitive interpretation of the information contained in table 1 is to view the numbers listed as the “uncertainty probability range” as confidence levels, with high numbers being desired. To drive the uncertainty estimation down, more Monte Carlo trials must be completed: the more Monte Carlo trials are done, the more certain the probability calculation. But to achieve an extremely low uncertainty, an unrealistic number of runs must be completed. The ideal situation in Monte Carlo analysis is to balance two considerations: a high confidence level with a low uncertainty level, and that the results be obtainable within reasonable time frames. This is the primary consideration in choosing the number of Monte Carlo trials to be run.

For this analysis, using table 1 determined that at least 900 runs of the software simulation needed to be performed to meet the reliability desired. Specifically, the results obtained in this analysis have a confidence level between 89.0 and 99.7 percent, with an uncertainty of 5 percent.

When the desired number of runs was determined, files were generated containing all relevant dispersions. Dispersion values were randomly selected from a normal distribution, and then stored in individual input files. This collection of files then was sequentially run from a main script, which directed the storage of relevant data. Additional scripts were written to process the data for analysis.

Because each simulation run lasted approximately 15 min and was recording large amounts of data, storing the relevant data for each flight without storing the entire data file generated by the simulation became necessary. For this reason, scripts were developed that took “snapshots” of the data at each flight phase. This snapshot process was performed on the entire data file after a run was completed. These scripts extracted the data at the beginning of each flight phase and directed the storage into separate and much smaller files. In this way, most of the data were discarded, and the process of completing many runs could be automated without exceeding memory limitations.

For the results shown in the next section, the X-33 simulation had all single-component dispersions randomly varied over a normal $3\text{-}\sigma$ distribution, no

[‡]Lintereur, Louis, “Basic Monte Carlo Analysis: The “Hit or Miss” Problem,” unpublished paper available from the author, 1999.

winds were present, and the RCS dispersions were turned off. A successful landing (or “hit”) was defined by three criteria: no loss of control, touchdown sink rates less than 6.0 ft/sec, and a touchdown equivalent airspeed between 160 and 190 kn.

Simulation Results and Conclusions Drawn

This section presents results for the 1000 Monte Carlo runs completed in this analysis. Selected results at touchdown are presented, as well as a discussion of two of the failed dispersion runs. Landing trajectories for several runs are also presented and discussed. Vehicle energy levels are correlated to the landing trajectories.

Selected Results at Touchdown

For the 1000 runs completed in this analysis, distribution plots of several variables at touchdown were examined. Distribution plots of equivalent airspeed and α at touchdown were used to determine whether or not the vehicle met the landing criteria constraints. Figure 3 shows that 46 of the 1000 cases (4.6 percent) did not meet the criterion that the landing speed be between 160 and 190 kn.

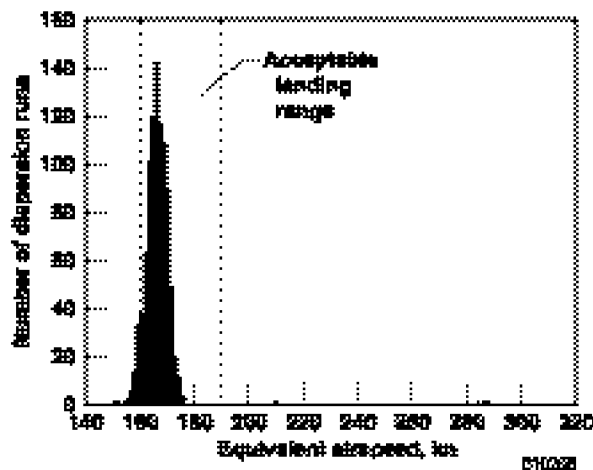


Figure 3. Equivalent airspeed at touchdown.

Figure 4 shows that the mean α at landing is 6.7° . Although the α value is not a specific landing criterion, large values for α would indicate an impending loss of control. Low values for α would indicate that forces on the nose gear might be too excessive for a landing without significant vehicle damage. The values seen for α in this analysis are reasonable and would not cause either a loss of control or excessive damage to the vehicle.

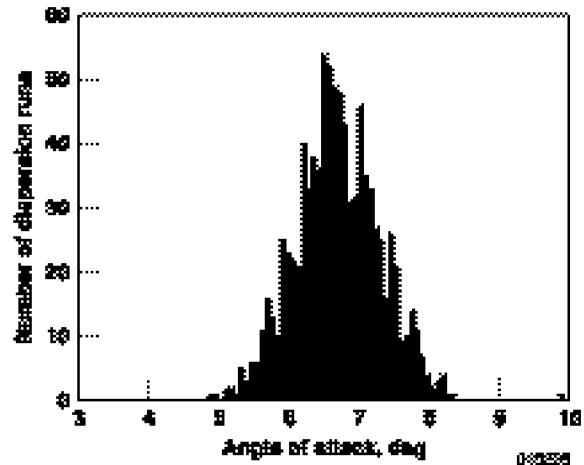


Figure 4. Angle of attack at touchdown.

Figure 5 shows the liquid oxygen weight at touchdown to approximately be between 240 and 290 lb. This range can be used to modify margins for possible trajectory modifications.

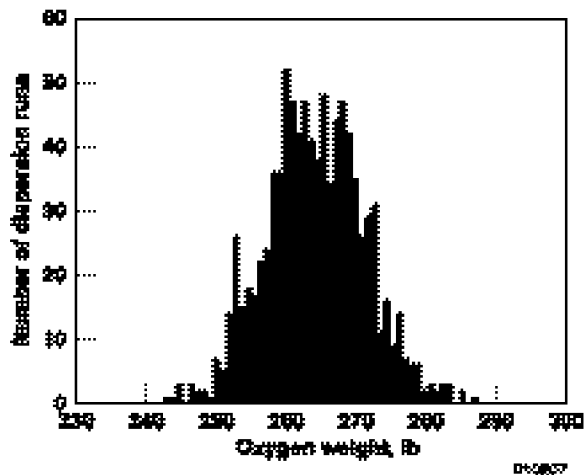


Figure 5. Liquid oxygen weight at touchdown.

Figure 6 shows the dispersion plot of lateral runway position at touchdown. The lateral position of the vehicle on the runway at landing is almost always located between 20 and 30 ft to the left of the runway center line, which was a known problem in the guidance portion of the software that was present in the software version used for this dispersion analysis. The runway coordinates contained in the guidance software were not aligned with the runway coordinates contained in the environmental model. This problem was to be corrected

in a later version of the X-33 simulation software. This example shows how the Monte Carlo dispersion analysis can be used to locate problems in the guidance or control portion of the software.

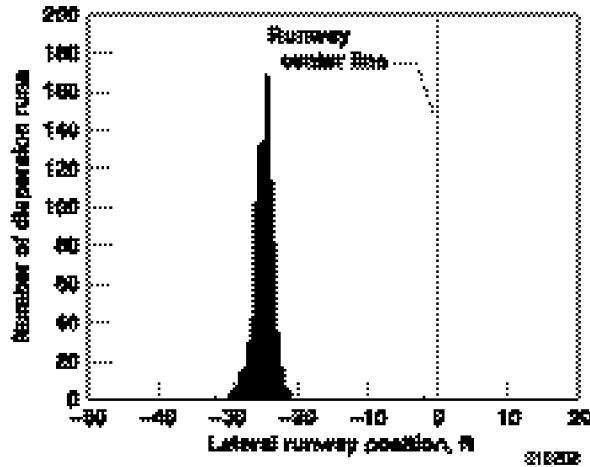


Figure 6. Lateral runway position at touchdown.

Examination of Failed Dispersion Runs

The examination of failed Monte Carlo dispersion runs provides useful information regarding individual dispersions and their effect on the flight of the vehicle. In one case, examination of a failed Monte Carlo dispersion run allowed for the determination of an individual dispersion to which the vehicle was particularly sensitive. The examination of another failed case provided a check on the magnitude of the 1- σ value on an individual dispersion. Both of these cases are discussed in the following section.

Correlating an Individual Dispersion to a Failed Monte Carlo Dispersion Run

During dispersion run number 797, a possibility of loss of control of the vehicle existed during ascent. Figure 7 shows that the possible loss of control occurs at approximately 241 sec. In this dispersion run, a 2.5432- σ dispersion value existed on pitching moment uncertainty. Although further analysis would need to be completed, this value is a preliminary indication that the vehicle may be sensitive to large pitching moment uncertainties. This example shows how the Monte Carlo dispersion runs can indicate which dispersion parameters will be more critical in flight. Further analysis can be conducted on individual dispersions to determine their effect on the vehicle (for example, how

large of a pitching moment uncertainty can be tolerated by the vehicle in ascent).

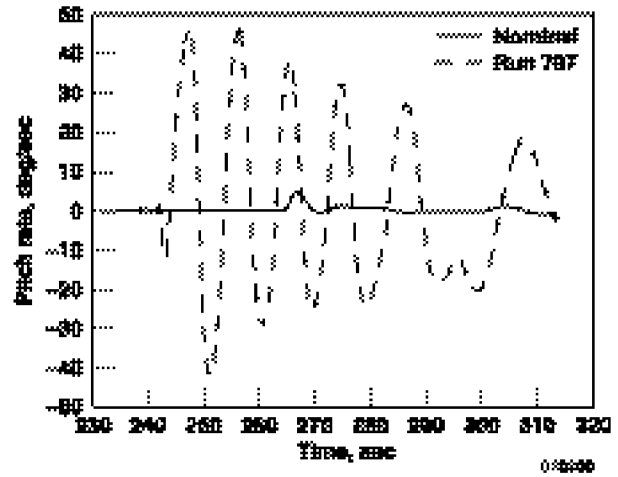


Figure 7. Pitch rate of dispersion run 797.

Accuracy of Dispersion Values

In dispersion run number 492, a spike in dynamic pressure is seen at approximately 450 sec (fig. 8). At this point in the flight, the loads and thermal parameter of dynamic pressure, q , times the value of α , in degrees, is on the order of 10^4 , which is well over the design limit. The vehicle was most likely lost at this point in the flight, although the simulation indicated a successful landing at 820.1 sec.

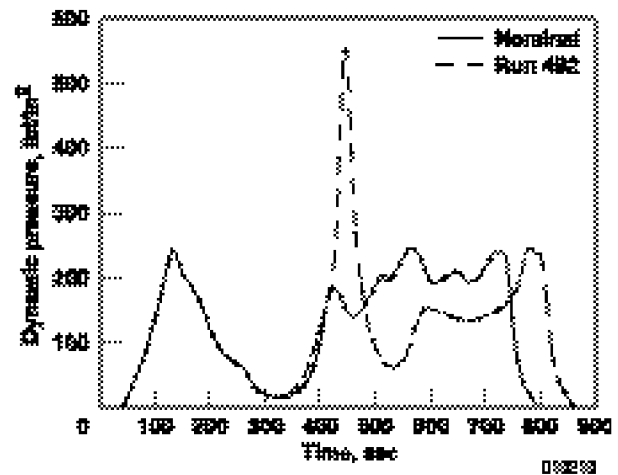


Figure 8. Dynamic pressure of dispersion run 492.

One unusually high dispersion value noted in this run was a $-3.2962\text{-}\sigma$ dispersion on x_{cg} . This offset of x_{cg} is the equivalent of moving the center of gravity 0.8 ft aft of the nominal x_{cg} position. The $1\text{-}\sigma$ dispersion value on x_{cg} (from just after main engine cutoff until landing) is 0.267 ft. This dispersion later was realized to have been accounted for in the mass properties dispersion model as well as in the propellant model—essentially, it was accounted for twice. Although this particular problem had been identified prior to the Monte Carlo dispersion runs (and was slated to be corrected in a future version), it is an example of how the examination of failed Monte Carlo dispersion runs can provide a check on the reasonableness and accuracy of the dispersion values quantified in the models.

Vehicle Trajectories and Energy

Examining vehicle trajectories and total energy levels during flight provides valuable information in determining whether the vehicle will land successfully and the type of trajectory needed to the landing site. For a nominal (that is, no dispersions present) run, the vehicle followed a ground track in a direct (straight) path to the landing site and then completed a counterclockwise 270-deg turn, called the heading alignment cone (HAC), before landing on the runway. Figure 9 shows this nominal landing trajectory.

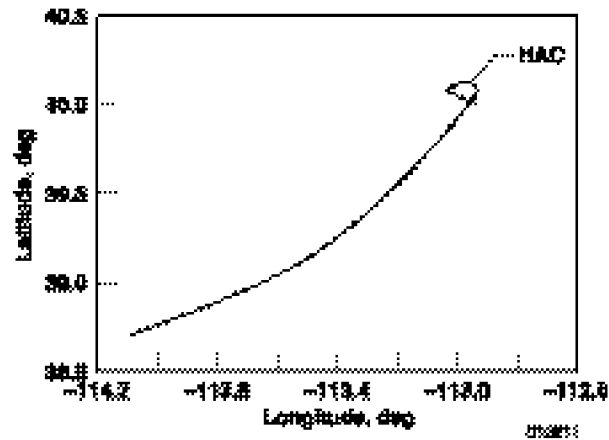


Figure 9. Landing trajectory for nominal run.

By examining the Monte Carlo runs and looking at the times of touchdown, some runs were seen to have very large touchdown times, as much as 300 sec longer than the nominal touchdown time. The vehicle was determined to have had excess amounts of energy, which took longer to dissipate before landing. Figure 10 shows an example of this excess energy in dispersion

run number 607. In this run, the vehicle successfully landed at 1034.0 sec (nominal landing time was 754.8 sec). The trajectory of run 607 is similar to the nominal trajectory, except that the HAC is 15–20 mi wider.

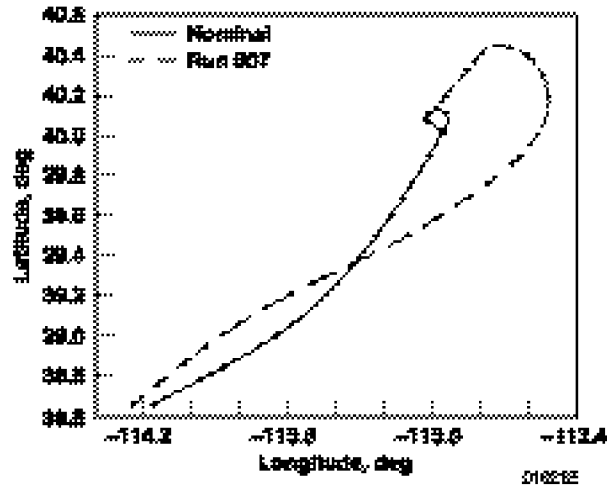


Figure 10. Landing trajectory of dispersion run 607.

Examining the energy state of the vehicle (eq. (1)) provides insight for this occurrence. Energy is calculated by summing up kinetic and potential energy of the vehicle:

$$E = \frac{1}{2}mv^2 + mgh \quad (1)$$

where E is the total energy of the vehicle, m is the mass of the vehicle, v is the velocity, g is the gravitational constant, and h is the altitude.

Figure 11 shows that the energy state of the vehicle in run 607 constantly was higher than the energy state of the vehicle during a nominal run. The vehicle lost energy by performing a wider turn for the HAC. Although the time of flight is significantly longer than in the nominal case (754.8 sec), the vehicle was able to complete a successful landing.

Other excess energy cases also had trajectories that were very interesting. Figure 12 shows one of the more unique landing trajectories seen in the 1000 Monte Carlo runs, dispersion run 145. The vehicle essentially completed two different HAC maneuvers in an attempt to lose enough energy for a landing: one in the counterclockwise (normal) direction and then one in the opposite direction before successfully landing.

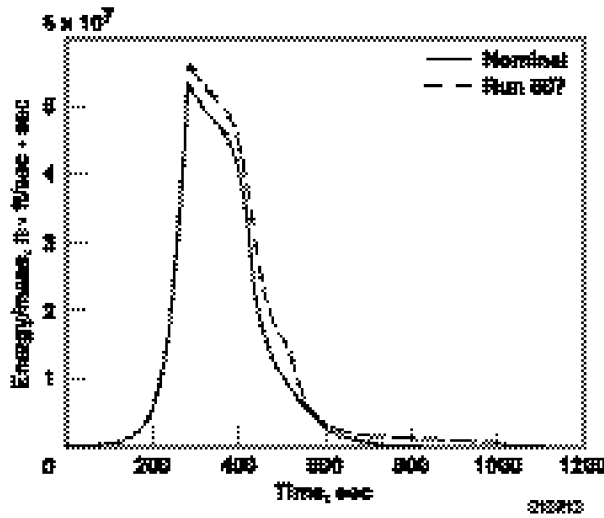


Figure 11. Energy state of dispersion run 607.

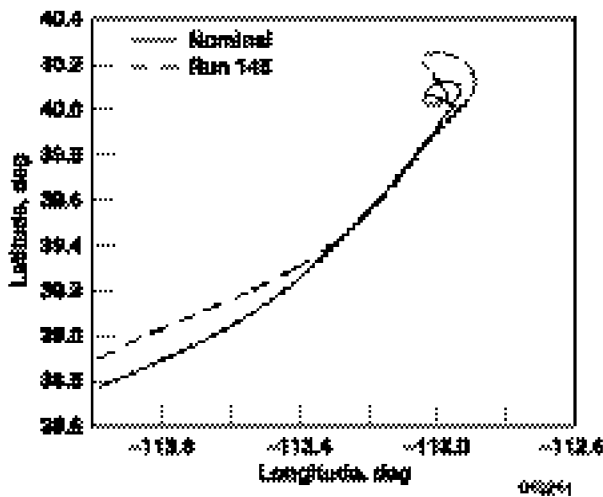


Figure 12. Landing trajectory of dispersion run 145.

Curiously enough, no cases existed of failed landings caused by energy higher than existed in the nominal landing case in the 1000 Monte Carlo runs. This fact may speak to the ability of the guidance algorithm to dissipate excess energy during flight for reasonable dispersion ranges.

Remarks

Funding was recently withdrawn from the X-33 project. Whether the program will continue under other funding is not known at this time. Thus, work on the Monte Carlo analysis tools for the X-33 simulation presently has been discontinued at NASA Dryden. If

work on the X-33 program resumes, future work will include additional Monte Carlo analysis on a final version of the flight software, as well as the examination of cases where a reconfigurable control system is implemented during flight and the effects on vehicle performance and stability are analyzed. A Monte Carlo dispersion analysis could be conducted on the reconfigurable control system, and the effects of the system on the vehicle flight and performance examined for additional information.

Summary

A Monte Carlo analysis of the X-33 software simulation was undertaken to show the usefulness of this type of analysis in the identification of design weaknesses in guidance or control, trajectory, and margins in specific aircraft parameters. Results were presented for selected conditions at touchdown and compared to the successful landing criteria for the vehicle. This Monte Carlo analysis showed that the vehicle did not meet the successful landing criteria in 4.6 percent of the 1000 cases.

Liquid oxygen weight margins at touchdown were presented to show that Monte Carlo dispersion analysis can be used to provide information for possible trajectory modifications. Using this analysis, liquid oxygen weight at vehicle touchdown was found to be between 240 and 290 lb. If determined to be necessary, this range could then be used to modify margins for possible trajectory modifications.

A dispersion plot of lateral runway position at touchdown was shown as an example of how the Monte Carlo dispersion analysis can uncover problems in the guidance portion of software. During this analysis, the software simulation was predicting a lateral touchdown position between 20 and 30 ft left of the runway center line, which was a known problem in the guidance portion of the software that was to be corrected in a later version of the software simulation. The Monte Carlo dispersion analysis was able to identify this known problem, showing the usefulness of this analysis technique.

In addition to determining mission success probability, a Monte Carlo dispersion analysis provides valuable information on vehicle parameters, as well as a way to verify that the simulation software itself is performing within defined limits. Landing trajectories for several runs were presented and discussed. Vehicle energy levels were correlated to the landing trajectories in a general sense. An extension of this work would

quantify the amounts of energy (that is, define energy “windows”) necessary at each flight phase for the vehicle to successfully land. Future work could also include alternate schemes to manage the vehicle energy—for example, considering vertical drops to lose energy (because of the shape and base drag of the X-33 vehicle) instead of using S-turns.

References

¹Freeman, Delma C., Theodore A. Talay, and R. Eugene Austin, *Reusable Launch Vehicle Technology Program*, NASA TM-110473, 1996.

²Justus, C. G., W. R. Jeffries III, S. P. Yung, and D. L. Johnson, *The NASA/MSFC Global Reference Atmospheric Model—1995 Version (GRAM-95)*, NASA TM-4715, 1995.

³Naftel, J. Christopher and Richard W. Powell, *Analysis of the Staging Maneuver and Booster Glideback Guidance for a Two-Stage, Winged, Fully Reusable Launch Vehicle*, NASA TP-3335, 1993.